Elements of dynamics of geometrically-accurate crossed-axes gear pair with line contact between the tooth flanks

Stephen Radzevich*

EATON Corp., Southfield Innovation Centre, Southfield, Michigan, USA

Abstract. The paper deals with geometrically-accurate crossed-axes gearing that features line contact between the tooth flanks of a gear, and of a mating pinion. The gearing of this design is commonly referred to « $R-gearing$ ». $R-gearing$ is the only possible kind of crossed-axes gearing, in which the tooth flanks of a gear, and of a mating pinion are in line contact with one another. Contact motion characteristics, and the key elements of dynamics of $R-gearing$ are concisely outlined in the paper. The tooth profile sliding, and sliding in the lengthwise direction of the gear tooth, are covered at the beginning of the paper in the section titled *Contact motion characteristics*. The key elements of dynamics of $R-gearing$ are discussed in the rest sections of the paper. Here, analytical solution to the problems under consideration is presented. The obtained results of the research are also valid for gear pairs that operate on intersected axes of rotation of a gear, and of a mating pinion. This becomes evident if one assumes the center-distance in the gear pair equal to zero. The discussed results of the research form a foundation for the further analysis of dynamics of real gear pairs that operate on crossing axes of rotation of a gear, and of a mating pinion.

1 Fundamentals of *R-gearing*

$R-gearing$ is a novel kind of gearing. Gearing of this design was invented by Prof. *S.P. Radzevich* at around ~2008. Since that time, the crossed-axes gearing of the proposed design was discussed in numerous papers that are available in the public domain [1-5], and others.

Despite of gearing itself, the key accomplishments in the field of $R-gearing$ are also extensively used in design of gear cutting tools for machining gears for $R-gear$ pairs [6], and others.

1.1 Principal kinematics of *R-gearing*

In a crossed-axes gear pair, a rotation, ω_p, from a driving shaft is transformed and transmitted to a rotation, ω_g, of a driven shaft by means of a driving pinion and a driven gear, as illustrated in Fig. 1. Three rotation vectors, namely, a rotation vector of the gear, $\boldsymbol{\omega}_g$, a rotation vector of a mating pinion, $\boldsymbol{\omega}_p$, and a vector of instantaneous rotation, $\boldsymbol{\omega}_{pl}$, of the pinion in relation to the gear, are used to construct a gear vector diagram. Here, (a) the rotation vector $\boldsymbol{\omega}_g$ is pointed along the gear axis of rotation, O_g, (b) the rotation vector $\boldsymbol{\omega}_p$ is pointed along the pinion axis of rotation, O_p, and (c) the rotation vector $\boldsymbol{\omega}_{pl}$ is pointed along the axis of instantaneous rotation, P_{ln}. The axes, O_g and O_p, are

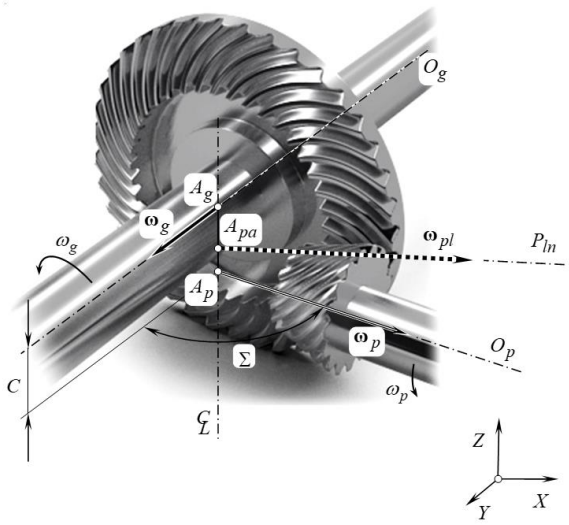

Fig. 1. Gear vector diagram of crossed-axes gear pair.

apart from one another at a center-distance, C. They form a shaft angle, Σ. Here, the shaft angle, Σ, is specified as $\Sigma = \angle(\boldsymbol{\omega}_g, \boldsymbol{\omega}_p)$. The gear base-cone-apex, the pinion base-cone-apex, and the plane-of-action apex, are designated as A_g, A_p, and A_{pa}, correspondingly. All of the apexes are situated within the center-line, $\mathcal{C}\!\!\!/$.

*Corresponding author: radzevich@usa.com

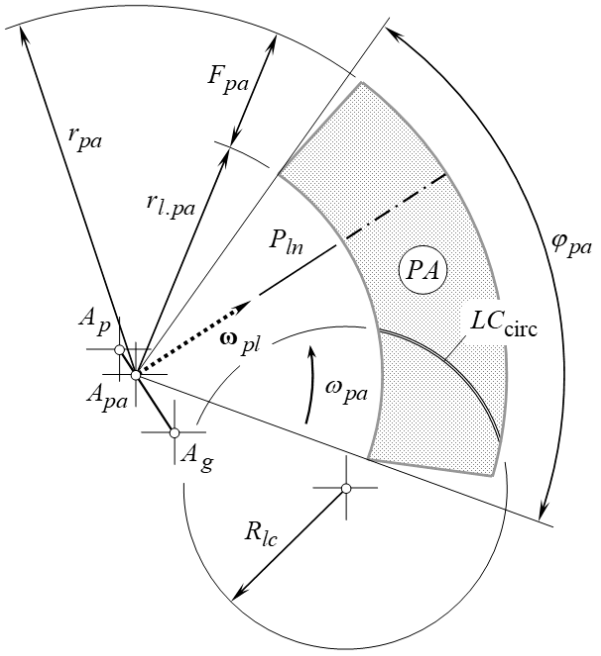

Fig. 2. Configuration of the desirable line of contact, LC_{circ}, within the plane of action, PA, in geometrically-accurate crossed-axes gear pair.

1.2 Tooth flank geometry in *R-gearing*

To generate tooth flanks, $\mathscr{G}$ and $\mathscr{P}$, of a gear, and of a mating pinion, in a crossed-axes gear pair, a desirable line of contact, LC_{des}, is used. The desirable line of contact, LC_{des}, is a planar curve that is entirely situated within the plane of action, PA. This curve is commonly specified in the reference system, $X_{pa}Y_{pa}Z_{pa}$, associated with the plane of action, PA. The desirable lines of contact, LC_{des}, of various geometries are used in present day practice: this could be a straight-line segment, a circular arc, LC_{circ} (see Fig. 2), an arc of cycloid, and so forth.

In a particular case of desirable line of contact in the form of straight-line segment, a line LC_{des}, of one of the following geometries can be employed:

- ✓ the line of contact of the base cone of the gear, and the plane of action (straight tooth gear is generated in this case); gear pair of this design is referred to as "*straight-gear* C_a *– gearing*"
- ✓ the line of contact of the base cone of the pinion, and the plane of action (straight tooth pinion is generated in this case); gear pair of this design is referred to as "*straight-pinion* C_a *– gearing*"
- ✓ the axis of instantaneous rotation, P_{ln} ; (neither straight tooth gear, nor straight tooth pinion is generated in this case); gear pair of this design is referred to as "*straight* C_a *– gearing*"

To generate the tooth flanks, $\mathscr{G}$ and $\mathscr{P}$, three main coordinate systems are employed. They are: (a) a *Cartesian* coordinate system, $X_gY_gZ_g$, associated with the gear, (b) a *Cartesian* coordinate system, $X_pY_pZ_p$, associated with the pinion, and (c) a *Cartesian* coordinate system, $X_{pa}Y_{pa}Z_{pa}$, associated with the plane of action, PA.

In the reference system, $X_{pa}Y_{pa}Z_{pa}$, position vector of point, $\mathbf{r}_{\text{des}}$, of the desirable line of contact, LC_{des}, is given by an equation in vector representation $\mathbf{r}_{\text{des}} = \mathbf{r}_{\text{des}}(u)$, where u is the parameter of the planar curve $\mathbf{r}_{\text{des}}$.

When the gears rotate, the desirable line of contact, LC_{des}, forms a family of consecutive positions in the reference systems, $X_gY_gZ_g$ and $X_pY_pZ_p$.

The position vector of point, $\mathbf{r}_g$, of the gear tooth flank, $\mathscr{G}$, is specified by a family of consecutive positions of the desirable line of contact, LC_{des}, given in the *Cartesian* coordinate system, $X_gY_gZ_g$:

$$\mathscr{G} \Rightarrow \mathbf{r}_g(u, \varphi_{pa}) = \mathbf{Rs}(pa \mapsto \mathscr{G}) \cdot \mathbf{r}_{\text{des}} \qquad (1)$$

Here, φ_{pa} is the angle of rotation of the plane of action, PA; $\mathbf{Rs}(pa \mapsto \mathscr{G})$ is the operator/matrix of the transition from the coordinate system, $X_{pa}Y_{pa}Z_{pa}$, to the gear coordinate system, $X_gY_gZ_g$.

The actual geometry of a geometrically-accurate gear for crossed-axes gear pair is illustrated in Fig. 3.

The position vector of point, $\mathbf{r}_p$, of the pinion tooth flank, $\mathscr{P}$, is specified by a family of consecutive positions of the desirable line of contact, LC_{des}, given in the *Cartesian* coordinate system, $X_pY_pZ_p$:

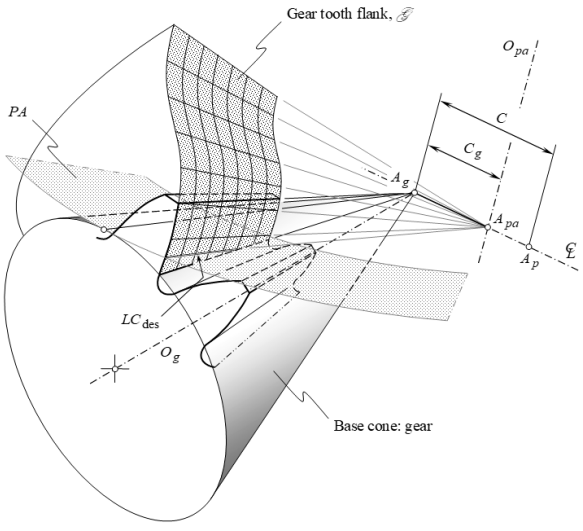

Fig. 3. Tooth flank, $\mathscr{G}$, in geometrically-accurate gear for C_a – axes gear pair.

$$\mathscr{P} \Rightarrow \mathbf{r}_p(u, \varphi_{pa}) = \mathbf{Rs}(pa \mapsto \mathscr{P}) \cdot \mathbf{r}_{\text{des}} \qquad (2)$$

Here, $\mathbf{Rs}(pa \mapsto \mathscr{P})$ is the operator/matrix of the transition from the coordinate system, $X_{pa}Y_{pa}Z_{pa}$, to the gear coordinate system, $X_pY_pZ_p$.

All three fundamental laws of gearing are met [3] if the tooth flanks fulfil Eq. (1) and Eq. (2).

2 Contact motion characteristics in *R-gearing*

Rotation of the input shaft, and rotation of the output shaft in a crossed-axes gear pair cause several other motions. Rolling and sliding of the tooth flanks are among these motions. Sliding is inevitable in crossed-axes gearing.

For better understanding of the nature of sliding, an in-detail investigation into the teeth sliding in geometrically-accurate crossed-axes gearing is required to be undertaken.

2.1 Tooth flank sliding in *R-gearing*

Sliding is inevitable in crossed-axes gearing. The velocity of sliding of tooth flanks in crossed-axes gearing can be viewed as a component of the velocity of the relative motion of the tooth flanks when the gears rotate.

In the particular case under consideration, it is convenient to interpret the plane of action, *PA* (see Fig. 4), as a driving component, and to consider both, the gear, and the pinion, as driven components.

Point m is an arbitrary point of the desirable line of contact, LC, between the tooth flanks, $\mathscr{G}$ and $\mathscr{P}$. The linear velocity vector of instantaneous motion of point m is designated as $\mathbf{V}_{m.pa}$. Considered in a reference system, associated with the gear, the projection of the linear velocity vector, $\mathbf{V}_{m.pa}$, onto the straight line that is tangent to LC at point m, equals to the linear velocity vector of the tooth flanks sliding in their lengthwise direction. This projection is entirely situated within the plane of action. Similarly, considered in that same reference system, the projection of the linear velocity vector, $\mathbf{V}_{m.pa}$, onto the straight line that is tangent to the tooth profile at point m, equals to the linear velocity vector of the tooth flanks sliding in their transverse section. This projection is entirely situated within the plane that is perpendicular to LC at point m.

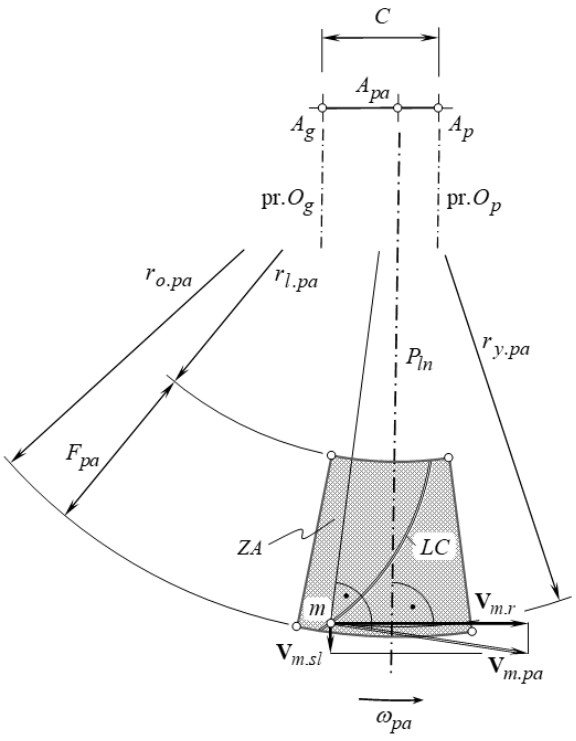

Fig. 4. Origination of axial sliding in geometrically-accurate crossed-axes gear pair.

In order to determine the sliding velocity in geometrically-accurate C_a – gearing, equations for the linear velocity vectors, $\mathbf{V}_{m.g}$ and $\mathbf{V}_{m.p}$, of point of interest, m, are required to be derived, and represented in a common reference system. A stationary *Cartesian* coordinate system, $X_{pa.s}Y_{pa.s}Z_{pa.s}$, associated with the plane of action, PA, is especially handy for solving the problem under consideration.

Operators of linear transformations are extensively used below for the derivation of analytical solution to the problem under consideration. The chief reason for that is as follows.

Commonly, it is convenient to derive an analytical expression for each of the linear velocity vectors, $\mathbf{V}_{m.g}$ and $\mathbf{V}_{m.p}$, in a specific reference system, and then to represent the derived equations in a common reference system. For instance, it is convenient to determine the linear velocity vector, $\mathbf{V}_{m.g}$, in a coordinate system associated with the gear. Similarly, it is convenient to determine the linear velocity vector, $\mathbf{V}_{m.p}$, in a coordinate system associated with the pinion. Later on, the derived equations for both the vectors, $\mathbf{V}_{m.g}$ and $\mathbf{V}_{m.p}$, can be represented in a common reference system. Use of operators of linear transformations, namely, the operators of translation, and of the operators of rotation, along and about the coordinate axes is proven to be helpful for this purpose.

Relative motion of a driving member, of a driven member in a gear pair, as well, as of the plane of action, form the foundation, on which the corresponding operators of the coordinate system transformations, $\mathbf{Rs}_{Ca}(g \to pa)$ and $\mathbf{Rs}_{Ca}(p \to pa)$, can be derived. When a gear pair operates, the driving member, the driven member, and the plane of action, all of them, are rotated in a timely manner, that is, the rotations, ω_g, ω_p and ω_{pa}, are synchronized with one another.

2.2 Sliding in the lengthwise direction of gear teeth

Sliding of two different kinds are distinguished when crossed-axes gearing operates. The tooth flank sliding in the lengthwise direction of the teeth is the first kind of sliding. The tooth flank sliding in the transverse direction of the teeth is the second kind of sliding.

Coordinate system transformations are extensively used in the analysis of sliding of a gear, $\mathscr{G}$, and of a mating pinion, $\mathscr{P}$, tooth flanks.

2.2.1 Analytical solution to the problem

For the analytical description of the linear transformation, namely, for the transition from the reference system, $X_g Y_g Z_g$, associated with the rotated gear, to the reference system, $X_{pa} Y_{pa} Z_{pa}$, associated with the rotated plane of action, PA, the operator, $\mathbf{Rs}_{Ca}(g \rightarrow pa)$, of the resultant coordinate system is used [3]. A similar operator of linear transformation, $\mathbf{Rs}_{Ca}(p \rightarrow pa)$, is derive for the pinion [3].

The operators of linear transformations, $\mathbf{Rs}_{Ca}(g \rightarrow pa)$ and $\mathbf{Rs}_{Ca}(p \rightarrow pa)$, are not presented here in expanded form, as both of them are bulky.

In the reference system, $X_g Y_g Z_g$, associated with the rotated gear, the linear velocity vector, $\mathbf{V}_{m.g}$, of point of interest, m, is analytically described by a column matrix:

$$\mathbf{V}_{m.g}\big|_g = \begin{bmatrix} -r_{b.g} \sin\varphi_g \\ r_{b.g} \cos\varphi_g \\ 0 \\ 1 \end{bmatrix} \tag{1}$$

To represent that same linear velocity vector, $\mathbf{V}_{m.g}$, in the coordinate system, $X_{pa} Y_{pa} Z_{pa}$, associated with the rotated plane of action, PA, the operator of linear transformation, $\mathbf{Rs}_{Ca}(g \rightarrow pa)$, is employed:

$$\mathbf{V}_{m.g}\big|_{pa} = \mathbf{Rs}_{Ca}(g \rightarrow pa) \cdot \mathbf{V}_{m.g}\big|_g \tag{2}$$

En equation that is similar to Eq. (1), is can be derived for the linear velocity vector, $\mathbf{V}_{m.p}$, of the rotated pinion.

$$\mathbf{V}_{m.p}\big|_{pa} = \mathbf{Rs}_{Ca}(p \rightarrow pa) \cdot \mathbf{V}_{m.p}\big|_p \tag{3}$$

Here, in Eq. (3), the operator, $\mathbf{Rs}_{Ca}(p \rightarrow pa)$, of the linear transformation is employed.

Consider relative motion of point within the line of contact of the tooth flanks, $\mathscr{G}$ and $\mathscr{P}$, of a gear, and of a mating pinion in a crossed-axes gear pair.

The vector, $\mathbf{V}_{rel}$, of relative motion of point of interest, m, equals to the difference:

$$\mathbf{V}_{rel} = \mathbf{V}_{m.p}\big|_{pa} - \mathbf{V}_{m.g}\big|_{pa} \tag{4}$$

where both the linear velocity vectors, $\mathbf{V}_{m.g}$ and $\mathbf{V}_{m.p}$, are represented in a common reference system, $X_{pa} Y_{pa} Z_{pa}$, associated with the rotated plane of action, PA.

These velocity vectors, $\mathbf{V}_{m.g}$ and $\mathbf{V}_{m.p}$, decisively affect the lubrication and friction parameters on the mating flanks and, hence, influence the load capacity and efficiency of the gear set.

In expanded form, the vector, $\mathbf{V}_{rel}$, can be represented in matrix form as:

$$\mathbf{V}_{rel}\big|_{pa} = \begin{bmatrix} V_{x.rel} \\ V_{y.rel} \\ V_{z.rel} \\ 1 \end{bmatrix} \tag{5}$$

The projection, $V_{y.rel}$, of the linear velocity vector, $\mathbf{V}_{rel}$, onto the axis, Y_{pa}, causes pure rolling of the gear and the mating pinion tooth flanks, $\mathscr{G}$ and $\mathscr{P}$, over each other. Therefore, this component of the linear velocity vector, $\mathbf{V}_{rel}$, is labeled below as $\mathbf{V}_{rol}$.

The projection, $V_{z.rel}$, of the linear velocity vector, $\mathbf{V}_{rel}$, onto the axis, Z_{pa}, causes profile sliding of the gear and the mating pinion tooth flanks, $\mathscr{G}$ and $\mathscr{P}$. Therefore, this component of the linear velocity vector, $\mathbf{V}_{rel}$, is labeled below as $\mathbf{V}_{sl.p}$.

The projection, $V_{x.rel}$, of the linear velocity vector, $\mathbf{V}_{rel}$, onto the axis, X_{pa}, causes *drag* sliding of the gear, and of the mating pinion tooth flanks, $\mathscr{G}$ and $\mathscr{P}$. Because of this, this component of the linear velocity vector, $\mathbf{V}_{rel}$, is labeled below as $\mathbf{V}_{sl.d}$.

Total sliding, $\mathbf{V}_{sl}$, in crossed-axes gearing can be calculated as the sum:

$$\mathbf{V}_{sl} = \mathbf{V}_{sl.p} + \mathbf{V}_{sl.d} \tag{6}$$

At different points within the zone of action, ZA, each of the components of the linear velocity vectors, namely, the vectors $\mathbf{V}_{sl}$, $\mathbf{V}_{sl.p}$, and $\mathbf{V}_{sl.d}$, vary.

A computer code for the calculation of all the components, $\mathbf{V}_{rol}$, $\mathbf{V}_{sl.p}$, and $\mathbf{V}_{sl.d}$, of the linear velocity vector, $\mathbf{V}_{rel}$, can be developed on the premise of the equations derived above in this section of the paper. Ultimately, the distribution of the components, $\mathbf{V}_{rol}$, $\mathbf{V}_{sl.p}$, and $\mathbf{V}_{sl.d}$, within the zone of action, ZA, in a crossed-axes gear pair can be interpreted graphically.

2.2.2 Specific sliding in geometrically-accurate crossed-axes gearing

For the specification of sliding between tooth flanks, $\mathscr{G}$ and $\mathscr{P}$, of a gear and of a mating pinion in crossed-axes gear pair, a dimensionless parameter is preferres to be used. This sliding parameter can be also

referred to as *specific sliding*. The *specific sliding* is denoted by γ_{Σ}. An actual value of *specific sliding* does not depend on rotation of the input/output shafts, and depends only on the design parameters of a gear, and of a mating pinion. The latter is especially important when optimizing the design parameters of gears in crossed-axes gear pairs.

Two different parameters, γ_{Σ}, are distinguished.

First, the slide/roll ratio for tooth flank, $\mathscr{G}$, of a gear. This ratio is calculated from a formula:

$$\gamma_{\Sigma.g} = \frac{V_{sl.g}^{m} - V_{sl.p}^{m}}{V_{sl.g}^{m}} \tag{7}$$

Second, the slide/roll ratio for tooth flank, $\mathscr{P}$, of a pinion. This ratio is calculated from a formula:

$$\gamma_{\Sigma.p} = \frac{V_{sl.p}^{m} - V_{sl.g}^{m}}{V_{sl.p}^{m}} \tag{8}$$

The calculation of sliding velocities, $V_{sl.g}^{m}$ and $V_{sl.p}^{m}$, in Eq. (7) and Eq. (8) is discussed immediately below.

In the reference system, $X_{pa}Y_{pa}Z_{pa}$, associated with the rotated plane of action, PA, the linear velocity vector, $\mathbf{V}_{m.g}\big|_{pa}$, can be represented in matrix form:

$$\mathbf{V}_{m.g}\big|_{pa} = \begin{bmatrix} V_{x.m.g} \\ V_{y.m.g} \\ V_{z.m.g} \\ 1 \end{bmatrix} \tag{9}$$

In a crossed-axes gear pair, the component, $V_{z.m.g}$, contributes to the profile sliding, and the component, $V_{x.m.g}$, contributes to the drag sliding (the component, $V_{y.m.g}$, contributes to pure rolling of the tooth flanks, $\mathscr{G}$ and $\mathscr{P}$). The sliding velocity, $V_{sl.g}^{m}$ [see Eq. (7) and Eq. (8)], can be expressed in terms of the velocities, $V_{x.m.g}$ and $V_{z.m.g}$, as:

$$V_{sl.g}^{m} = \sqrt{V_{x.m.g}^{2} + V_{z.m.g}^{2}} \tag{10}$$

Similarly, in the reference system, $X_{pa}Y_{pa}Z_{pa}$, associated with the rotated plane of action, PA, the linear velocity vector, $\mathbf{V}_{m.p}\big|_{pa}$, can be represented in the form of column mantrix:

$$\mathbf{V}_{m.p}\big|_{pa} = \begin{bmatrix} V_{x.m.p} \\ V_{y.m.p} \\ V_{z.m.p} \\ 1 \end{bmatrix} \tag{11}$$

In a crossed-axes gear pair, the component, $V_{z.m.p}$, contributes to the profile sliding, and the component, $V_{x.m.p}$, contributes to sliding in the lengthwise direction of the gear tooth (the component, $V_{y.m.p}$, contributes to pure rolling of the tooth flanks, $\mathscr{G}$ and $\mathscr{P}$). The sliding velocity, $V_{sl.p}^{m}$, can be expressed in terms of the velocities, $V_{x.m.p}$ and $V_{z.m.p}$, as:

$$V_{sl.p}^{m} = \sqrt{V_{x.m.p}^{2} + V_{z.m.p}^{2}} \tag{12}$$

The sliding velocities, $V_{sl.g}^{m}$ and $V_{sl.p}^{m}$ [see Eq. (10), and Eq. (12)], can be entered into the expressions:

$$\gamma_{\Sigma.g} = \frac{V_{sl.g}^{m} - V_{sl.p}^{m}}{V_{sl.g}^{m}} \tag{13}$$

$$\gamma_{\Sigma.p} = \frac{V_{sl.p}^{m} - V_{sl.g}^{m}}{V_{sl.p}^{m}} \tag{14}$$

to calculate the specific roll/slide ratios, $\gamma_{\Sigma.g}$ and $\gamma_{\Sigma.p}$, in crossed-axes gearing.

The specific sliding, γ_{Σ}, is of a positive value on the addendum portions of the tooth flanks. The parameter, γ_{Σ}, does not exceed 1. At points within the axis of instantaneous rotation, P_{ln}, specific sliding, γ_{Σ}, is equal to zero, and it is equal to 1 at the base cone of the mating gear.

The specific sliding on the dedendum portion of the tooth flanks is of a negative value. It is equal to zero at points within the axis of instantaneous rotation, P_{ln}, and it approaches a minus infinity at the base cone.

The specific roll/slide ratios, $\gamma_{\Sigma.g}$ and $\gamma_{\Sigma.p}$, can be plotted within the zone of action, ZA, as only the region, ZA, of the plane of action comes into effect when investigating the engagement of the gear teeth.

2.2.3 Features of specific sliding in geometrically-accurate crossed-axes gearing

The interaction of the tooth flanks, $\mathscr{G}$ and $\mathscr{P}$, in geometrically-accurate crossed-axes gearing features sliding in the lengthwise direction of gear teeth (see Fig. 4). Therefore, in addition to specific roll/slide ratios, $\gamma_{\Sigma.g}$ and $\gamma_{\Sigma.p}$ [see Eq. (7) and Eq. (8)], two more characteristics are required to be introduced to specify specific sliding in crossed-axes gear pairs.

Specific profile roll/slide ratios, $\gamma_{p.g}$ and $\gamma_{p.p}$, are the first additional characteristics. These two ratios are specified as:

$$\gamma_{p.g} = \frac{V_{z.m.g} - V_{z.m.p}}{V_{z.m.g}} \tag{15}$$

$$\gamma_{p.p} = \frac{V_{z.m.p} - V_{z.m.g}}{V_{z.m.p}} \tag{16}$$

Specific roll/slide ratios, $\gamma_{d.g}$ and $\gamma_{d.p}$, for the sliding in the lengthwise direction of the gear teeth are the second additional characteristics. These two ratios are specified as:

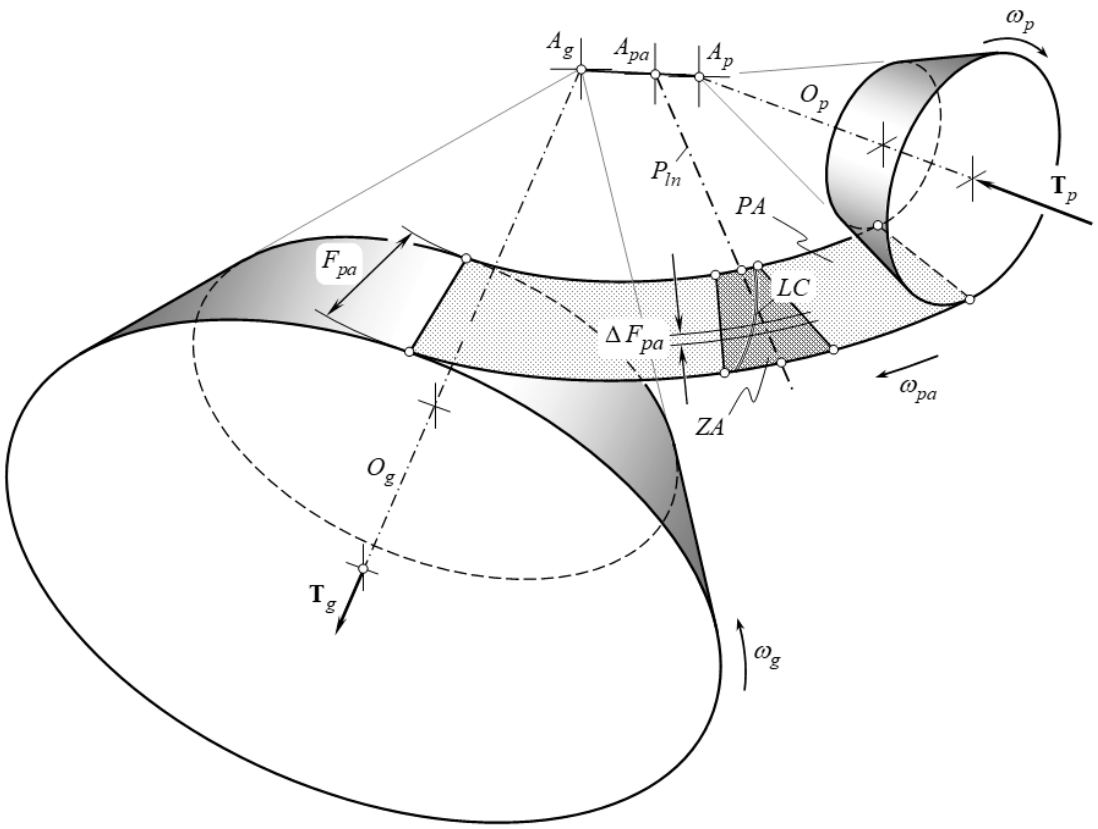

Fig. 5. Schematic for calculation of forces that act in geometrically-accurate crossed-axes gear pair.

$$\gamma_{d.g} = \frac{V_{x.m.g} - V_{x.m.p}}{V_{x.m.g}} \tag{17}$$

$$\gamma_{d.p} = \frac{V_{x.m.p} - V_{x.m.g}}{V_{x.m.p}} \tag{18}$$

Specific profile roll/slide ratios, $\gamma_{p.g}$ and $\gamma_{p.p}$, and specific drag roll/slide ratios, $\gamma_{d.g}$ and $\gamma_{d.p}$, are helpful for more in-detail analysis of sliding conditions in crossed-axes gearing.

It is right point to turn the readers' attention here to that that gears with a low tooth count are more vulnerable to sliding between the tooth flanks, $\mathscr{G}$ and $\mathscr{P}$. They are also more sensitive to the variation of the roll/slide conditions within the zone of action, ZA.

3 Elements of dynamics of geometrically-accurate crossed-axes gearing

In a crossed-axes gear pair, the input shaft, and the output shaft, are loaded by an input torque, and by output torque, correspondingly. As the gears interact with one another, a force of the interaction is exerted from the driving member of the gear pair. An actual value of the force of interaction, as well, as the components of this force, depend on the input torque, and on the design parameters of the gear, and of the mating pinion. Considering an input torque, and an input rotation of constant values (namely, no acceleration/deceleration is taken into account in the performed below analysis), it is required to determine the forces that act between a gear, and a mating pinion in a crossed-axes gear pair

3.1 The principal assumption adopted in the load analysis of *R-gearing*

When a crossed-axes gear pair operates, the tooth flanks, $\mathscr{G}$ and $\mathscr{P}$, of the gear and that of the mating pinion, interact with one another at points within the line(s) of contact, LC. The line(s) of contact is entirely situated within the plane of action, PA. This makes possible a conclusion that the force of interaction between the tooth flanks, $\mathscr{G}$ and $\mathscr{P}$, acts along a straight line that is also entirely located within the plane of action, PA.

As the line of action of the force is entirely situated within the plane of action, PA, then the following assumption seems to be reasonable in the load analysis of geometrically-accurate crossed-axes gearing.

Referring to Fig. 5, consider base cones of a gear, and of a mating pinion, along with the plane of action. The gear is rotated, ω_g, about its axis of rotation, O_g, and the pinion is rotated, ω_p, about its axis of rotation, O_p, as schematically illustrated in Fig. 5. The plane of action, PA, is in tangency to both the base cones. The plane of action, PA, rotates, ω_{pa}, about its axis of

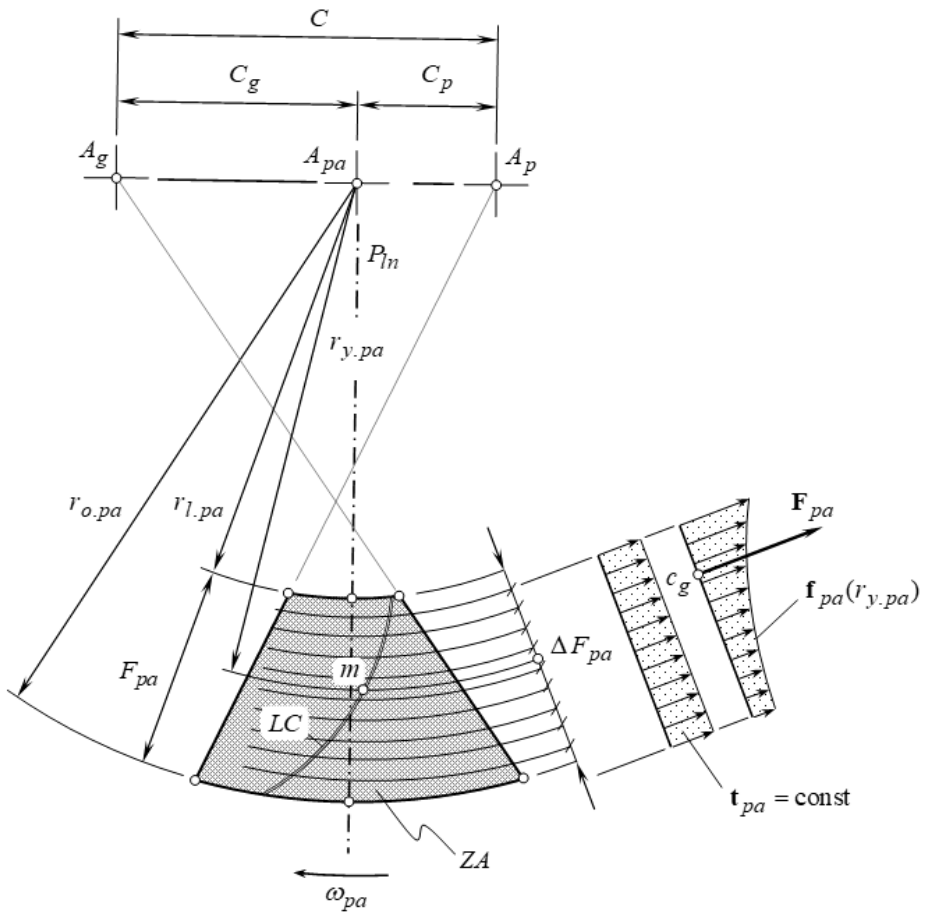

Fig. 6. Forces acting in geometrically-accurate crossed-axes gear pair.

rotation (not shown in Fig. 5) that passes through the *plane-of-action apex*, A_{pa}, and is pointed perpendicular to the plane of action. It is instructive to point out here that in contrast to the *equivalent pulley-and-belt transmission*, where the belt ***pools*** the driven member, in reality, in a gear pair, the driving gear ***pushes*** the driven member. In this way, the direction of the rotation, ω_{pa}, is specified in Fig. 5.

The rotations, ω_g, ω_p, and ω_{pa}, are synchronized with one another so, as to fulfil the equations:

$$\frac{\omega_g}{\omega_{pa}} = \sin\Gamma_b\,; \quad \frac{\omega_p}{\omega_{pa}} = \sin\gamma_b\,; \quad \frac{\omega_g}{\omega_p} = \frac{\sin\Gamma_b}{\sin\gamma_b} \tag{19}$$

The input torque, $\mathbf{T}_p$, is applied to the pinion shaft, and the output torque, $\mathbf{T}_g$, is applied to the gear shaft. The torque, $\mathbf{T}_{pa}$, is a *virtual* parameter. This torque is applied to the rotated plane of action, PA. The ratios of the magnitudes, T_g, T_p, and T_{pa}, of the torques, $\mathbf{T}_g$, $\mathbf{T}_p$, and $\mathbf{T}_{pa}$, are inverse to the corresponding ratios of the rotations, ω_g, ω_p, and ω_{pa}:

$$\frac{T_g}{T_{pa}} = \frac{1}{\sin\Gamma_b}\,; \quad \frac{T_p}{T_{pa}} = \frac{1}{\sin\gamma_b}\,; \quad \frac{T_g}{T_p} = \frac{\sin\gamma_b}{\sin\Gamma_b} \tag{20}$$

Interaction between a gear tooth flank, $\mathscr{G}$, and a mating pinion tooth flank, $\mathscr{P}$, occurs only within the zone of action, ZA. Width of the zone of action is designated as F_{pa}. Width of the zone of action, F_{pa}, is calculated as the difference $F_{pa} = r_{o.pa} - r_{l.pa}$ between the outer, $r_{o.pa}$, and the inner, $r_{l.pa}$, radii of the active portion of the plane of action, PA (see Fig. 6).

The interaction between the tooth flanks, $\mathscr{G}$ and $\mathscr{P}$, is observed only along a line(s) of contact, LC (or portions of the lines of contact), those situated within the zone of action, ZA. There are one or two (and not more than three) lines of contact (portions of the lines of contact) within the zone of action, ZA, effective simulataneously. In crossed-axes gear pairs of a special design the total number of the lines of contact can be greater than three.

A gear, and a mating pinion in a crossed-axes gear pair can be sliced onto a large enough number, N_{sl}, of slices, each of which is perpendicular to the gear axis of rotation, O_g, and to the pinion axis of rotation, O_p, correspondingly. It is handy to illustrate the slicing of a gear pair using the plane of action, PA, for this purpose. The thickness of the slices is designated as ΔF_{pa}. It is calculated as:

$$\Delta F_{pa} = \frac{F_{pa}}{N_{sl}} \tag{21}$$

In the best-case scenario, the slice thickness approaches to a zero ($\Delta F_{pa} \to 0$), and the number of the slices approaches an infinity ($N_{sl} \to \infty$). In this latter case, the slice thickness is denoted by dF_{pa}. It is assumed here and below that the torque being transmitted by each of the slices is equal to one another. Considering the plane-of-action torque, $\mathbf{T}_{pa}$, the following expression:

$$\mathbf{t}_{pa} = \frac{\mathbf{T}_{pa}}{F_{pa}} = \text{const} \tag{22}$$

can be composed for a torque per unit length, $\mathbf{t}_{pa}$.

Similar equations:

$$\mathbf{t}_g = \frac{\mathbf{T}_g}{F_{pa}} = \text{const}\,; \quad \mathbf{t}_p = \frac{\mathbf{T}_p}{F_{pa}} = \text{const} \tag{23}$$

are valid with respect to the gear, as well, as to the mating pinion.

As the torque per unit length, $\mathbf{t}_{pa}$, is of a constant value, and the equality, $\mathbf{t}_{pa}F_{pa} = \mathbf{T}_{pa}$, is valid, then the actual value of the plane-of-action torque, $\mathbf{T}_{pa}$ (lumped torque), is proportional to the shadowed area in Fig. 6.

Equal torque share among the slices is graphically illustrated in Fig. 6.

In order to transmit a given power, it is always desirable to design and to implement gearboxes of the smallest possible size. From this perspective, the active portion of the line of contact, LC, should begin from the *plane-of-action apex*, A_{pa}. Evidently, the line of contact of such a geometry is far from to be practical, as the maximum contact and bending strength of the gear teeth is restricted by physical properties of a material the gear and the mating pinion are made of.

Calculation of the design parameters of the favorable portion of the line of contact is based on the assumption that the power being transmitting by a gear pair is equally shared within active portion of the gear pair face width. With that said, under the torque of a constant value, the smaller diameter of a gear/pinion, the large the force, and vice versa. Therefore, a practical value of the smallest possible diameter of the gear/pinion is limited by the yield contact and bending stress in the gear tooth.

The above discussion makes reasonable the following assumption:

Assumption 1: *In a crossed-axes gear pair, the torque per unit length, $\mathbf{t}_{pa}$, is equally shared in the radial direction among an infinite number of infinitesimally narrow slices, each of which is perpendicular to the axis of rotation either of the plane of action, or of the gear, or of the pinion.*

This assumption is referred to as the *first fundamental assumption* in dynamics of crossed-axes gearing

The first fundamental assumption is derived on the premis of the mandatory equilibrium of the adjacent infinitesimally narrow strips of the plane of action, PA, which must be stationary in relation to one another (and, thus, are not allowed traveling with respect to each other).

A similar assumption has been made with respect to parallel-axes gear pairs, as well, as with respect to intersected-axes gearing.

3.2 Forces of the interaction in geometrically-accurate crossed-axes gearing

The forces that act in a geometrically-accurate crossed-axes gear pair are considered below in different reference systems. The analysis begins with the load applied within the plane of action, PA. Then, this analysis enhanced to the forces that act on the bearings, on the gear housing, and so forth.

3.2.1 Total force acting in geometrically-accurate crossed-axes gearing

In the plane-of-action, PA, the torque, $\mathbf{T}_{pa}$, creates the plane-of-action tangential force, $\mathbf{F}_{pa}$. The tangential force per unite length, $\mathbf{f}_{pa}$, can be expressed in terms of the torque per unit length, $\mathbf{t}_{pa}$, and the distance, $r_{y.pa}$, of a given slice from the plane-of-action apex, A_{pa}, as:

$$\mathbf{f}_{pa} = \frac{\mathbf{t}_{pa}}{r_{y.pa}} \tag{24}$$

It is instructive to point out here that the tangential force per unite length, $\mathbf{f}_{pa}$, is a function of the distance, $r_{y.pa}$, of point of interest, m, from the plane-of-action apex, A_{pa}, that is: $\mathbf{f}_{pa} = \mathbf{f}_{pa}(r_{y.pa})$.

The distribution of the tangential force per unite length, $\mathbf{f}_{pa}(r_{y.pa})$, in the radial direction of the plane of action is illustrated in Fig. 6.

Having the tangential force per unite length, $\mathbf{f}_{pa}$, determined, the total tangential forth, $\mathbf{F}_{pa}$, is calculated from the expression:

$$\mathbf{F}_{pa} = F_{pa}\cdot\mathbf{f}_{pa} + \mathbf{t}_{pa}\int_{r_{l.pa}}^{r_{o.pa}} \frac{1}{r_{y.pa}}\,dr_{y.pa} =$$

$$= F_{pa}\cdot\mathbf{f}_{pa} + \mathbf{t}_{pa}\cdot\left(\ln|r_{o.pa}| - \ln|r_{l.pa}|\right) \tag{25}$$

$$\mathbf{F}_{pa} = F_{pa}\cdot\mathbf{f}_{pa} + \mathbf{t}_{pa}\cdot\ln\left|\frac{r_{o.pa}}{r_{l.pa}}\right| \tag{26}$$

The similar equations:

$$\mathbf{F}_g = F_{pa}\cdot\mathbf{f}_g + \mathbf{t}_g\cdot\ln\left|\frac{r_{o.pa}}{r_{l.pa}}\right| \tag{27}$$

$$\mathbf{F}_p = F_{pa} \cdot \mathbf{f}_p + \mathbf{t}_p \cdot \ln \left| \frac{r_{o.pa}}{r_{l.pa}} \right|$$

are valid with respect to the gear, as well, as to the mating pinion.

The total (lumped) forth, $\mathbf{F}_{pa}$, is applied at point, c_g, within the line of contact, LC, that is remote from the plane-of-action apex, A_{pa}, at distance, r_{cg} (see Fig. 6).

Transmission of a rotation from a driving shaft to a driven shaft is due to the tangential forth, $\mathbf{F}_{pa}$, that acts between the tooth flanks, $\mathscr{G}$ and $\mathscr{P}$, of the mating gears.

When the gears rotate, friction is observed between the gear tooth flank, $\mathscr{G}$, and the mating pinion tooth flank, $\mathscr{P}$. The friction between the compressed gear and pinion tooth flanks, $\mathscr{G}$ and $\mathscr{P}$, is due to the sliding that occurs between the tooth flanks, $\mathscr{G}$ and $\mathscr{P}$. As it is already shown earlier, sliding of two types are distinguished in crossed-axes gear pairs. The profile sliding is the first kind, and the sliding in the lengthwise direction of the gear teeth is the second kind of sliding in crossed-axes gearings. Therefore, friction forces of two types have to be recognized, namely, the profile friction force, $\mathbf{F}_{pr}$, and the friction force in the lengthwise direction, $\mathbf{F}_{dr}$. These friction forces contribute to the total force of the interaction, $\mathbf{F}_{\Sigma}$, between the gear tooth flank, $\mathscr{G}$, and the mating pinion tooth flank, $\mathscr{P}$:

$$\mathbf{F}_{\Sigma} = \mathbf{F}_{pa} + \mathbf{F}_{pr} + \mathbf{F}_{dr} \qquad (29)$$

The component, $\mathbf{F}_{pa}$, is specified by Eq. (26).

In the reference system, $X_{pa}Y_{pa}Z_{pa}$, associated with the rotated plane of action, PA, the profile (transverse) friction force, $\mathbf{F}_{pr}$, is pointed along the axis Z_{pa}, as illustrated in Fig. 7. The actual value of this force equals $\mathbf{F}_{pr} = \mu_{pr} \cdot \mathbf{F}_{pa}$. Here, μ_{pr} designates the coefficient of friction in profile sliding of the gear, $\mathscr{G}$, and of the pinion, $\mathscr{P}$, tooth flanks.

In that same reference system, $X_{pa}Y_{pa}Z_{pa}$, the friction force in the lengthwise direction, $\mathbf{F}_{dr}$, is pointed along the axis X_{pa}. The actual value of this component equals (see Fig. 7) $\mathbf{F}_{dr} = \mu_{dr} \cdot \mathbf{F}_{pa}$. The coefficient of friction in "*drag*" sliding of the gear, $\mathscr{G}$, and of the pinion, $\mathscr{P}$, tooth flanks is denoted by μ_{dr}.

The coefficients of friction, μ_{pr} and μ_{dr}, can be of different values, as the normal curvatures of the gear and of the pinion tooth flanks, $\mathscr{G}$ and $\mathscr{P}$, at point of interest are significantly different in the transverse, and in the lengthwise directions of the tooth flanks $\mathscr{G}$ and $\mathscr{P}$. Moreover, the conditions of profile (transverse) sliding, and that in the lengthwise direction of the gear teeth, are also different. However, when performing a preliminary analysis, the coefficients of friction, μ_{pr} and μ_{dr}, can be considered equal to one another ($\mu_{pr} = \mu_{dr}$).

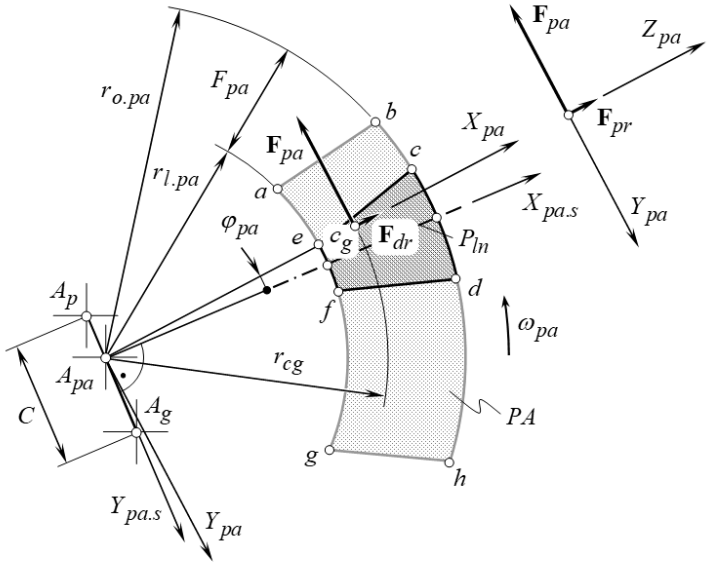

Fig. 7. Tangential force, $\mathbf{F}_{pa}$, and friction forces, $\mathbf{F}_{pr}$ and $\mathbf{F}_{dr}$, in crossed-axes gear pair.

The total friction force (lumped force), $\mathbf{F}_{fr.\Sigma}$, in geometrically-accurate crossed-axes gearing is calculated as:

$$\mathbf{F}_{fr.\Sigma} = \mathbf{F}_{pr} + \mathbf{F}_{dr} \qquad (30)$$

The friction forces, $\mathbf{F}_{pr}$ and $\mathbf{F}_{dr}$, in a crossed-axes gear pair are negligibly small, and, thus, commonly they are not taken into account when calculating the design parameters of the gear transmission. Moreover, the friction forces, $\mathbf{F}_{pr}$ and $\mathbf{F}_{dr}$, do not affect the uniformity of the output rotation in a gear pair, as both, $\mathbf{F}_{pr}$ and $\mathbf{F}_{dr}$, act along the straight lines that are entirely situated within a plane that is perpendicular to the plane of action, PA (and that is tangent to the gear, $\mathscr{G}$, and the pinion, $\mathscr{P}$, tooth flanks at point of interest, m). Only component of the total force of interaction, $\mathbf{F}_{\Sigma}$, that is pointed along the common perpendicular to the tooth flanks, $\mathscr{G}$ and $\mathscr{P}$, causes a rotation of the driven gear in a crossed-axes gear pair.

Different components of the total tangential force, $\mathbf{F}_{pa}$, of interaction between the tooth flanks, $\mathscr{G}$ and $\mathscr{P}$, of a gear and of a mating pinion, along with the forces $\mathbf{F}_g$ and $\mathbf{F}_p$ that act on the gear and the pinion, are entered into equations for the calculation of the bending, and of the contact strength of the gear and of the pinion teeth, the bearings, the housing, the shafts, and so forth.

The forces that act on the gear, have to be expressed in a stationary coordinate system, $X_{g.s}Y_{g.s}Z_{g.s}$, associated with the motionless gear (that is, associated with the gear pair housing).

After the total tangential force, $\mathbf{F}_{pa}$, of interaction between the tooth flanks, $\mathscr{G}$ and $\mathscr{P}$, of a gear, and of a mating pinion, has been pre-multiplied by the operator of the linear transformation, $\mathbf{Rs}_{Ca}(pa \rightarrow g_s)$, the total force, $\mathbf{F}_{g.s}$, that acts over the gear can be represented in the form of a column matrix:

$$\mathbf{F}_{g.s} = \mathbf{Rs}(pa \rightarrow g_s) \cdot \mathbf{F}_{pa} = \begin{bmatrix} F_{x.g.s} \\ F_{y.g.s} \\ F_{z.g.s} \\ 1 \end{bmatrix} \tag{31}$$

The components $F_{x.g.s}$, $F_{y.g.s}$, and $F_{z.g.s}$, of the total force, $\mathbf{F}_{g.s}$, in Eq. (31) are equal to the separating force, $F_{g.sep}$, the tangential force, $F_{g.tg}$, and the axial thrust, $F_{g.ax}$, correspondingly, that is, the equalities $F_{x.g.s} = F_{g.sep}$, $F_{y.g.s} = F_{g.tg}$, and $F_{z.g.s} = F_{g.ax}$, are valid. The forces, $\mathbf{F}_{g.sep}$, $\mathbf{F}_{g.tg}$, and $\mathbf{F}_{g.ax}$, are entered into the equations for the calculation of the design parameters of a gearbox.

3.2.2 Forces acting on the gear and the pinion in geometrically-accurate crossed-axes gearing

In a reference system, $X_{pa}Y_{pa}Z_{pa}$, associated with the rotated plane of action, PA, the orientation of the force, $\mathbf{F}_{pa}$ [namely, of the force specified by Eq. (26)], or of the total force, $\mathbf{F}_{\Sigma}$ [that is specified by Eq. (29)], does not alter when the gears rotate. However, actual configuration of the coordinate system, $X_{pa}Y_{pa}Z_{pa}$, in relation to a motionless reference system, associated with the gear pair housing, alters when the gears rotate. Therefore, in a stationary coordinate system, $X_{g.s}Y_{g.s}Z_{g.s}$, associated with the motionless gear, Eq. (31) has to be rewritten in a form:

$$\mathbf{F}_{g.s}(\varphi_g) = \begin{bmatrix} F_{g.sep}(\varphi_g) \\ F_{g.tg}(\varphi_g) \\ F_{g.ax}(\varphi_g) \\ 1 \end{bmatrix} \tag{32}$$

As it follows from the analysis of Eq. (32), the total lumped force, $\mathbf{F}_{g.s}$, as well, as all three components, $\mathbf{F}_{g.sep}$, $\mathbf{F}_{g.tg}$, and $\mathbf{F}_{g.ax}$, that act over the gear, depend on the angle of rotation of the gear, that is, all of them are functions the angle, φ_g, of rotation of the gear:

$$\begin{aligned} \mathbf{F}_{g.s} &= \mathbf{F}_{g.s}(\varphi_g) & \mathbf{F}_{g.tg} &= \mathbf{F}_{g.tg}(\varphi_g) \\ \mathbf{F}_{g.sep} &= \mathbf{F}_{g.sep}(\varphi_g) & \mathbf{F}_{g.ax} &= \mathbf{F}_{g.ax}(\varphi_g) \end{aligned} \tag{33}$$

The lumped force, $\mathbf{F}_{g.s}(\varphi_g)$, and the components, $\mathbf{F}_{g.sep}(\varphi_g)$, $\mathbf{F}_{g.tg}(\varphi_g)$, and $\mathbf{F}_{g.ax}(\varphi_g)$, that depend on the angular parameter, φ_g, are additional sources of vibration generation, and noise excitation in crossed-axes gearing. When the gears rotate, point of intersection of the axis of instantaneous rotation, P_{ln}, and the instantaneous line of action, LA_{inst}, are not allowed to migrate along the axis of instantaneous rotation, P_{ln}, or, at least, the distance, covered in this migration, has to be the shortest possible. It is desirable to design gears so, as to minimize the travel distance along the axis of instantaneous rotation.

The variation of the direction of the (total) lumped force, $\mathbf{F}_{g.s}(\varphi_g)$, of interaction of tooth flanks, $\mathscr{G}$ and $\mathscr{P}$, of a gear and of a mating pinion is illustrated in Fig. 8. For an arbitrary configuration of the line of contact, LC, between the tooth flanks, $\mathscr{G}$ and $\mathscr{P}$, the coordinates of point, c_g, at which the total force, $\mathbf{F}_{g.s}$, is applied, can be determined. The component, $\mathbf{F}_{g.ax}$, is

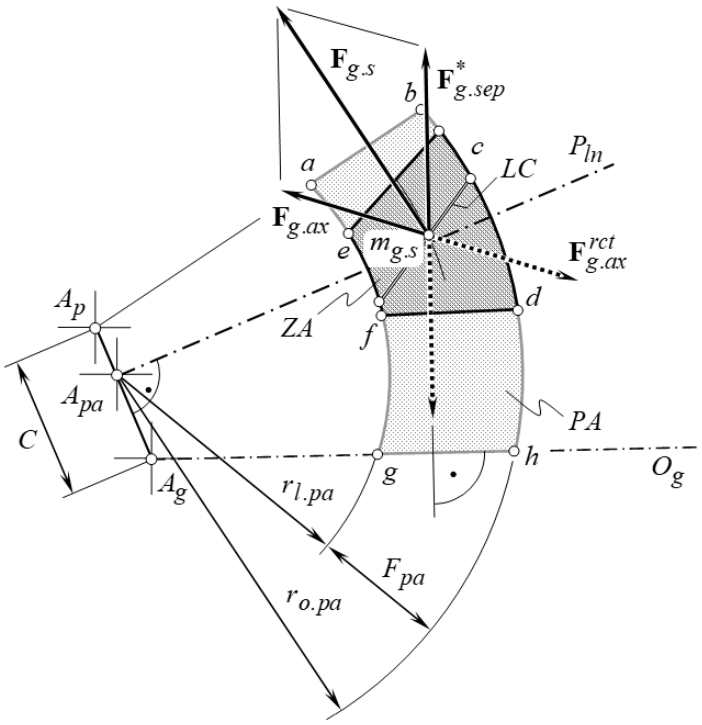

Fig. 8. The axial thrust, $\mathbf{F}_{g.ax}(\varphi_g)$, and the separating force, $\mathbf{F}_{g.sep}(\varphi_g)$, as the components of the resultant (lumped) force, $\mathbf{F}_{g.s}(\varphi_g)$, of interaction of the tooth flanks, $\mathscr{G}$ and $\mathscr{P}$, of a gear, and of a mating pinion in geometrically-accurate crossed-axes gear pair.

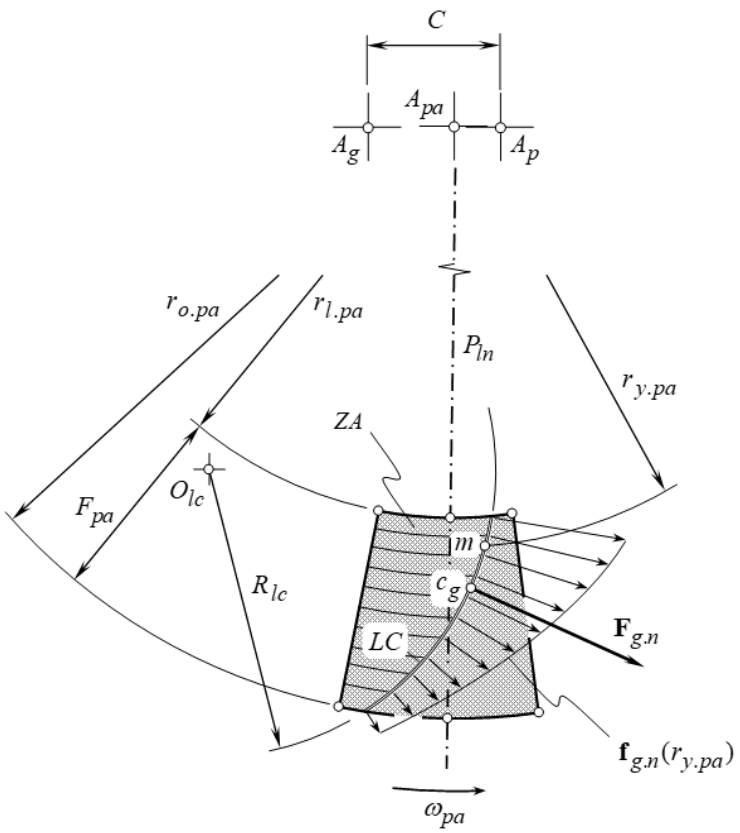

Fig. 9. Lumped normal force, $\mathbf{F}_{g.n}$, and normal force per unit length, $\mathbf{f}_{g.n}$, acting in geometrically-accurate crossed-axes gear pair.

parallel to the gear axis of rotation, O_g. The component, $\mathbf{F}_{g.sep}$, is perpendicular to the gear axis of rotation, O_g. The magnitude, $F^*_{g.sep}$, of the shown in Fig. 9 the force vector, $\mathbf{F}^*_{g.sep}$, equals to $F^*_{g.sep} = F_{g.sep}/\sin\phi_{t.\omega}$, where $\phi_{t.\omega}$ is the transverse pressure angle in the crossed-axes gear pair. (The separating force vector, $\mathbf{F}_{g.sep}$, is entirely situated in the normal $N_{ln}-$plane. The normal plane (the $N_{ln}-plane$) is the plane through the plane-of-action-apex, A_{pa}, perpendicular to the center-line, $\mathbb{C}$, in the gear pair. As it follows from the analysis of the schematic shown in Fig. 9, at any configuration of the line of contact, LC, for which the point, c_g, is situated within the zone of action, ZA, the forces, $\mathbf{F}_{g.ax}$ and $\mathbf{F}_{g.sep}$, never equals to zero. Thus, the reaction forces, $\mathbf{F}^{rct}_{g.ax}$ and $\mathbf{F}^{rct}_{g.sep}$, also are of non-zero values. As the forces, $\mathbf{F}^{rct}_{g.ax}$ and $\mathbf{F}^{rct}_{g.sep}$, fluctuate when the gears rotate [see Eqs. (33)], an excessive vibration generation, and noise excitation can be observed when a crossed-axes gear pair operates. The variation of the forces, $\mathbf{F}^{rct}_{g.ax}$ and $\mathbf{F}^{rct}_{g.sep}$, does not depend on the geometry of the line of contact, LC. This discussion is also valid in cases, when multiple lines of contact, as well, as multiple portion of the lines of contact, are observed in a gear pair of a particular design, as the forces, $\mathbf{F}^{rct}_{g.ax}$ and $\mathbf{F}^{rct}_{g.sep}$, fluctuate when the gears rotate. Fluctuation of the forces, $\mathbf{F}^{rct}_{g.ax}$ and $\mathbf{F}^{rct}_{g.sep}$, is inevitable in geometrically-accurate crossed-axes gear pairs.

An analysis, similar to the aforementioned one, can be performed with respect to loading of the pinion in a geometrically-accurate crossed-axes gear pair.

As it follows from the analysis of Eq. (34), the resultant lumped force, $\mathbf{F}_{p.s}$, as well, as all three components, $\mathbf{F}_{p.sep}$, $\mathbf{F}_{p.tg}$, and $\mathbf{F}_{p.ax}$, that act over the pinion, depend on the angle of rotation of the pinion, that is, all of them are functions the angle, φ_p, of rotation of the pinion:

$$\mathbf{F}_{p.s} = \mathbf{F}_{p.s}(\varphi_p) \qquad \mathbf{F}_{p.tg} = \mathbf{F}_{p.tg}(\varphi_p)$$
$$\mathbf{F}_{p.sep} = \mathbf{F}_{p.sep}(\varphi_p) \qquad \mathbf{F}_{p.ax} = \mathbf{F}_{p.ax}(\varphi_p) \tag{34}$$

The lumped force, $\mathbf{F}_{p.s}(\varphi_p)$, and the components, $\mathbf{F}_{p.sep}(\varphi_p)$, $\mathbf{F}_{p.tg}(\varphi_p)$, and $\mathbf{F}_{p.ax}(\varphi_p)$, that depend on the angular parameter, φ_p, are an additional source of vibration generation, and noise excitation in crossed-axes gearing. When the gears rotate, no migration of point of intersection of the axis of instantaneous rotation, P_{ln}, as well, as of the instantaneous line of action, LA_{inst}, along the axis of instantaneous rotation, P_{ln}, is allowed (or, at least, the distance covered in this migration has to be the shortest possible). It is desirable to design gears so, as to minimize the travel distance along the axis of instantaneous rotation.

For any configuration of the line of contact, LC, when the point, c_g, is situated within the zone of action, ZA, the forces, $\mathbf{F}_{p.ax}$ and $\mathbf{F}_{p.sep}$, never equal to zero. Thus, the reaction forces, $\mathbf{F}^{rct}_{p.ax}$ and $\mathbf{F}^{rct}_{p.sep}$, also are of non-zero values. As the forces, $\mathbf{F}^{rct}_{p.ax}$ and $\mathbf{F}^{rct}_{p.sep}$, fluctuate when the gears rotate, an excessive vibration generation, and noise excitation are commonly observed when a crossed-axes gear pair operates. The variation of the forces, $\mathbf{F}^{rct}_{p.ax}$ and $\mathbf{F}^{rct}_{p.sep}$, does not depend on the geometry of the line of contact, LC. This discussion is also valid with respect to the cases when multiple lines of contact, as well, as multiple portion of the lines of

contact, are observed in a gear pair of a particular design, as the fluctuation of the forces, $\mathbf{F}_{p.ax}^{rct}$ and $\mathbf{F}_{p.sep}^{rct}$, is inevitable in geometrically-accurate crossed-axes gear pairs.

3.2.3 Normal force acting on the gear in geometrically-accurate crossed-axes gearing

For the calculations of gear teeth for contact strength, as well, as for contact strength analysis, a component, $\mathbf{F}_{g.n}$, of the total forth, $\mathbf{F}_{g.s}$, is entered into the corresponding equations for the calculations. This component is commonly referred to as the *normal force*, $\mathbf{F}_{g.n}$. The vector of normal load, $\mathbf{F}_{g.n}$, is situated within the plane of action, PA, and is perpendicular to the line of contact, LC, at point, c_g, at which the normal load is applied. The magnitude, $F_{g.n}$, of the normal force, $\mathbf{F}_{g.n}$, is calculated from the expression $F_{g.n} = F_{g.s}\cos\psi_g$, where ψ_g is the actual value of the spiral angle of the gear teeth at point, c_g.

The normal force per unit length, $\mathbf{f}_{g.n}$, is also entirely situated within the plane of action, PA. The normal force per unit length, $\mathbf{f}_{g.n}$, depends on the geometry of a particular line of contact. At every point of the line of contact, LC, the applied normal load per unit length, $\mathbf{f}_{g.n}$, is perpendicular to the line of contact at that point.

In straight bevel gearing, the normal force per unit length, $\mathbf{f}_{g.n}$, is distributed similar in much to that shown in Fig. 6 for the force per unit length, $\mathbf{f}_{pa}(r_{y.pa})$. In skew crossed-axes gearing, the normal force per unit length, $\mathbf{f}_{g.n}$, is distributed similar to that in straight bevel gearing – all the elementary forces are perpendicular to the line of contact, LC. The distribution of the normal force per unit length, $\mathbf{f}_{g.n}$, in spiral bevel gearing with a circular-arc line of contact, LC, of a radius, R_{lc}, is illustrated in Fig. 9. In this particular case, all the elementary forces are pointed along the radius, R_{lc}, to the corresponding point, m, within the line of contact, LC.

In a more general case of geometrically-accurate crossed-axes gearing, in face-hobbed bevel gears in particular, the following approach can be used to determine the distribution of the normal force per unit length along the line of contact, LC.

First, the unit normal vector, $\mathbf{n}_{lc}$, is constructed at every point of the line of contact, LC.

Second, the distribution of the normal load per unit length, $\mathbf{f}_{g.n}$, is constructed as a product of the unit vector, $\mathbf{n}_{lc}$, by the function of the distribution of the magnitude, $f_{g.n}$, of the normal load per unit length, that is, $\mathbf{f}_{g.n} = f_{g.n} \cdot \mathbf{n}_{lc}$.

When two, or more lines of contact (or portions of the line of contact), LC_i, are observed, then positon vector, $\mathbf{r}_{cg.\Sigma}$, of the point, $c_{g.\Sigma}$, at which the resultant load, $\mathbf{F}_{g.n.\Sigma}$, is applied, can be calculated from the formula:

$$\mathbf{r}_{cg.\Sigma} = \frac{\sum\limits_{i} l_{lc.i} \cdot \mathbf{r}_{cg.i}}{\sum\limits_{i} l_{lc.i}} \tag{35}$$

where:

i – is the number of lines of contact (or portions of line of contact), LC_i

$l_{lc.i}$ – is the length of line of contact (or a portions of a line of contact), LC_i

$\mathbf{r}_{cg.i}$ – is the position vector of point, $c_{g.i}$, of a line of contact (or a portion of a line of contact), LC_i

$\sum\limits_{i} l_{lc.i}$ – is the total length, $TLLC$, of all the lines of contact, $l_{lc.i}$

The variation of the direction of the total lumped force of the interaction of the tooth flanks, $\mathscr{G}$ and $\mathscr{P}$, can be minimized by means of selection of the desirable line of contact, LC_{des}, of proper geometry. When the gears rotate, point of intersection of the axis of instantaneous rotation, P_{ln}, and the line along the total force of interaction of the tooth flanks, $\mathscr{G}$ and $\mathscr{P}$, are not allowed to migrate along the P_{ln}, or, at least, the distance of this migration has to be minimized. In this way, the vibration generation, and noise excitation can be minimized.

3.2.4 Cases of multiple lines of contact

Gear pairs of all designs feature the contact ratio greater than one ($\bar{m} > 1$). The contact ratio in the range of $\bar{m} = 1.4 \ldots 1.8$ is common in preset-day parctice.

As the inequalty, $\bar{m} > 1$, is always valid, periods of gear meshing when eithe one, or two (or more), portions of the line of contact are occur.

When a single line of contact is observed, the entire load is transmitted through this line of conact between the interacting tooth flanks, $\mathscr{G}$ and $\mathscr{P}$.

When two (or more), portions of the line of contact are observed, the active lines of contact share the load being transmitted by the gear teeth.

The load carrying capacity of a gear pair depends on the manner the load is shared between the lines of contact.

Consider an active portion of the plane of action, PA, in a geometrically-accurate crossed-axes gear pair, as illustrated in Fig. 10. In this schematic, an arbitrary point of interest, m_i, is chosen within an arbitrary line of

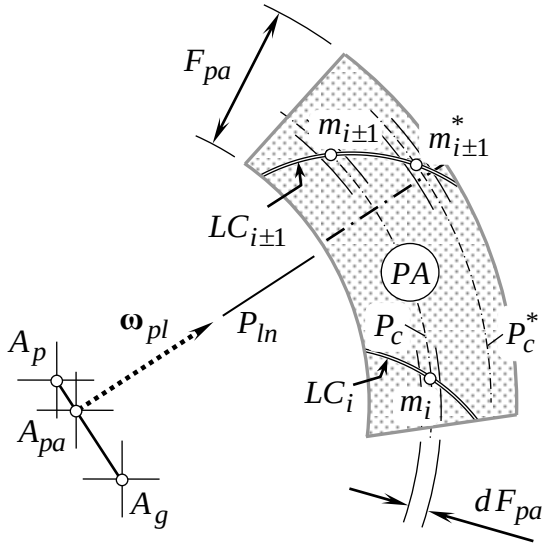

Fig. 10. Case of multiple lines of contact.

contact, LC_i. When the gears rotate, point m_i traces the path of contact, P_c. The path of contact, P_c, intersects the adjacent line of contact, $LC_{i\pm1}$, at point, $m_{i\pm1}$. At a certain instant of time, contact in the gear pair occurs in both points, m_i and $m_{i\pm1}$, at that same time. In such a scenario, the load to be transmitted is equally shared between the loacal arcs of the lines of contact in differential vicinity of contact points, m_i and $m_{i\pm1}$. In cases of multiple lines of contact, the load to be transmitted by a gear pair is shared equally among all the active pairs of teeth (proportionally to the actual number of tooth pairs involved in mesh).

In contrast to the path of contact, P_c, when the gears rotate, another point, $m^*_{i\pm1}$, of the line of contact traces another path of contact, P^*_c. The path of contact, P^*_c, does not intersect any other line of contact between the tooth flanks, $\mathscr{G}$ and $\mathscr{P}$. In this scenario, the entire load is transmitted by a local portion of the arc of the line of contact within the differential vicinity of the contact point, $m^*_{i\pm1}$. This load is twice as big compared to the load, shared in the previous case.

The performed analysis allows the following assumption:

Assumption 2: *The load to be transmitted by a gear pair is shared equally among the all active pairs of teeth (proportionally to the actual number of tooth pairs involved in mesh).*

This assumption is commonly referred to as the *second fundamental assumption* in dynamics of crossed-axes gearing

This assumption is derived on the premis of equilibrium of the adjacent infinitesimally narrow strips of the plane of action, PA, which must be stationaly in relation to one another (and, thus, are not allowed traveling with respect to each other).

The greater the contact ratio in a gear pair, the better the load share among the tooth pairs, and vice versa.

4 Conclusions

The paper deals with geometrically-accurate crossed-axes gearing having line contact between the tooth flanks of the gear, and of the mating pinion. Gearing of this particular design is commonly referred to "$R-gearing$".

In the first section of the paper, fundamentals of $R-gearing$ are briefly outlined. Actually, the principal kinematics of $R-gear\ pairs$, along with the tooth flank geometry of the mating gears, are covered in this section of the paper.

Contact motion characteristics in $R-gearing$ are discussed in the second section of the paper. A gear, and a mating pinion tooth flanks sliding are considered. This section of the paper ends with the analysis of specific sliding, and features of the specific sliding, in $R-gearing$.

Elements of dynamics of geometrically-accurate crossed-axes gearing are disclosed in the third section of the paper. This section begins with the first principal assumption adopted in the load analysis of $R-gearing$, and is followed by the analysis of forces of interaction in geometrically-accurate crossed-axes gearing. This includes, but is not limited to: (a) Total force acting in geometrically-accurate crossed-axes gearing; (b) Forces acting on the gear, and the pinion, in geometrically-accurate crossed-axes gearing; and (c) Normal forces acting on the gear, and the pinion, in geometrically-accurate crossed-axes gearing. The case of multiple lines of contact in $R-gear\ pairs$ got special consideration. Here, in this sub-section, the second principal assumption that is adopted in the load analysis of $R-gearing$ is introduced.

References

1. Radzevich, S. P. "On fundamentals of the scientific theory of gearing". – in: *Power Transmissions*, Proceedings of the 4th International Conference, held at Sinaia, Romania, June 20-23, 2012, Editor: George Dobre, Assisted by Mihai Robert Vladu, Mechanism and Machine Science, Vol. 13, Springer, 2013, pp.165-172.
2. Radzevich, S.P., "*R*-Gearing: A Novel Kind of Crossed-Axis Gearing having Line Contact between the Tooth Flanks of the Gear and of the Pinion", In: Proceedings of *International Conference on Gears*, October 7-9, 2013, Technical University of Munich (TUM), Garching (Near Munich), Germany, 2013, pp.1303-1314. (Volume 2).
3. Radzevich, S.P., *Theory of Gearing: Kinematics, Geometry, and Synthesis*, 2nd Edition, revised and expanded, *CRC* Press, Boca Raton, FL, 2018, 934 pages.

4. Radzevich, S.P., "Design Features of Perfect Gears for Crossed-Axes Gear Pairs", *Gear Solutions*, February, 2019, pp. 36-43.
5. Radzevich, S.P., "Conjugate Action Law in Intersected-Axes Gear Pairs and in Crossed-Axes Gear Pairs", *Gear Solutions* magazine, June 2020, pages 42-48.
6. Radzevich, S.P., *Gear Cutting Tools*: *Science and Engineering*, 2nd Edition, CRC Press, Boca Raton, FL, 2017, 606 pages.

Bibliography

Radzevich, S.P., (Editor), *Advances in Gear Design and Manufacture*, CRC Press, Boca Raton, Florida, 2019, 549 pages.

Radzevich, S.P., "An Examination of High-Conformal Gearing", *Gear Solutions*, February, 2018, pages 31-39.

Radzevich, S.P., (Editor), *Dudley's Handbook of Practical Gear Design and Manufacture*, 4th edition, *CRC* Press, Boca Raton, FL, 2021, 1170 pages, 718 B/W Illustrations.

Radzevich, S.P., *High-Conformal Gearing: Kinematics and Geometry*, 2nd Edition, Elsevier, Amsterdam, 2020, 506 pages.

Radzevich, S.P., "Knowledge (of Gear Theory) is Power in the Design, Production, and Application of Gears", *Gear Solutions* magazine, August 2020, pages 38-44. [Upon request, a .pdf of this article can be ordered (for free) from the author].

Radzevich, S.P., *Theory of Gearing: Kinematics, Geometry, and Synthesis*, 3rd Edition, *CRC* Press, Boca Raton, FL, 2022, 1128 pages.

Radzevich, S.P., (Editor), *Novikov/Conformal Gearing: Scientific Theory and Practice*, Springer, 1st ed., 2023 Edition, 505 pages.

Radzevich, S.P., (Editor), *Recent Advances in Gearing: Scientific Theory and Applications*, Springer, 1st ed., 2022 Edition, 569 pages.

Radzevich, S.P., Storchak, M.G. (Editors), *Advances in Gear Theory and Gear Cutting Tool Design*, Springer, 2022, 500 pages.